Journal of Physics: Theories and Applications E-ISSN: 2549-7324 / P-ISSN: 2549-7316
J. Phys.: Theor. Appl. Vol. 2 No.02 (2018) 43-52 doi: 10.20961/jphystheor-appl.v2i2.30664

Precursor concentration effect on optical properties of carbon dots from Cassava's peels

Permono Adi Putro[1], Liszulfah Roza[1], and Isnaeni[2]

[1]Physics Education, Faculty of Teacher Education and Science, University of Muhammadiyah Prof. Dr. Hamka, Pasar Rebo, East Jakarta 130830 Indonesia

[2]Research Center for Physics, Indonesia Institute of Science, Building 442, Puspitek Serpong, South Tangerang, Banten 15314 Indonesia

Email : [1]permonoadi29@gmail.com

Received 22 July 2018, Revised 23 August 2018, Published 30 September 2018

Abstract: Carbon dots (C-dots) are a new type of fluorescent nanoparticles that can be readily synthesized from natural sources, such as cassava's peels. In this work, C-dots were synthesized from cassava's peels using low temperature green synthesis based. The Green synthesis techniques were done by using water as a solvent non-chemical and natural sources. The Synthesis was done using various concentrations of precursor from 0.25%, 0.50%, 1.0% and 2.0%. Optical properties of C-dots were characterized using spectrophotometer UV-Vis, photoluminescence (PL) and time resolved photoluminescence (TRPL). The concentration of precursor lead to differences in molecular density and content of preparation thus affecting optical properties. The performance of C-dots optical properties were dominated by the transition of electrons n–π* on structure aromtic C=O which originate from the surface of C-dots. The result of C-dots sample with a concentration of 2.0% precursors has the best emission effiency. This provides the potential for C-dots cassava's peels in the aqueous solution to be applied as cellular bioimaging and biosensing metal ions and salts.

Keyword : C-dots, concentration of precursor, optical properties

1. Introduction

Fullerens are molecules of carbon atoms arranged like balls with 0 dimensions and in a discrete energy state (Neto, Guinea, Peres, Novoselov, & Geim, 2009). Carbon dots (C-dots) represent a newly emerging class of fluorescence materials and provide extensive applications in various biomedical and optoelectronic fields comparable to conventional inorganic semiconductors that eco-friendly and can be controlled (Dimos, 2016; Hola et al., 2014). C-dots have a diameter below 10 nm. C-dots which smaller than Bohr's radius can be luminescent when the quantum confinement effect dominates. The distribution of heterogeneous sizes of C-dots conjugated sp^2 in a sp^3 matrix non-conjugated to produce discrete energy levels that lead to very different optical, electrical, and chemical properties compared to other nanoparticles (Hassan, Gomes, Dehghani, & Ardekani, 2018).

C-dots can be synthesized using two different methods; the approach of top down and bottom up usually consists of elements such as carbon, hydrogen, and oxygen. Atoms such as nitrogen, boron, sulfur, etc. can be filled in through the appropriate doping method that it changes its properties (Jaleel & Pramod, 2018). Nanoparticle synthesis by breaking down large particles into nanometer-sized particles is called the method top-down. Top-down methods include the method of arc discharge, laser ablation, electrochemical oxidation, chemical oxidation,and ultrasonic synthesis. The method bottom-up uses atoms or molecules that form the desired nanometer-sized particles, such as microwave synthesis, thermal decomposition, hydrothermal treatment, templated routes, and plasma treatment (Baker & Baker, 2010; Goryacheva, Sapelkin, & Sukhorukov, 2017; Hu, Gong, Liu, & Choi, 2017; Liu, Zhao, & Zhang, 2014; R. Wang, Lu, Tang, & Xu, 2017). Simple and fast C-dots synthesis techniques are constantly being developed, such as simple heating using an oven and based on green synthesis.

The development of making C-dots using natural materials that have carbon chain bonds is a challenge and the progress is very rapid (Baker & Baker, 2010; Ma, Dong, Sun, & Chen, 2017; Ngu, Chia, Fong, & Ng, 2016). However, the optical properties of C-dots from natural resources or chemicals have comparable purity (Isnaeni, Rahmawati, Intan, & Zakaria, 2018). Some previous studies have used natural ingredients as C-dots, namely orange peel (Fatimah, Isnaeni, & Tahir, 2018), ginger and galangal (Isnaeni et al., 2018), grape pulp (Varisco et al., 2017), sweet potato (Shen, Shang, Chen, Wang, & Cai, 2017), sweet pepper (Yin et al., 2013), strawberry (Huang et al., 2013), strawberry (Huang et al., 2013). However, no one has used the source of cassava's peels to C-dots using the low temperature technique. In this study, we will use variations in concentration precursor to study its effect on the optical properties of C-dots.

2. Research Methods

The basic ingredient used for the synthesis of C-dots is cassava's peels which obtained from the local market of Lembang, Ciledug, Tangerang City, Indonesia. Water is used as a non-chemical solvent in methods green synthesis using low temperature. The mechanism of C-dots synthesis using low temperature is carried out through several steps which can be seen in Figure 1.

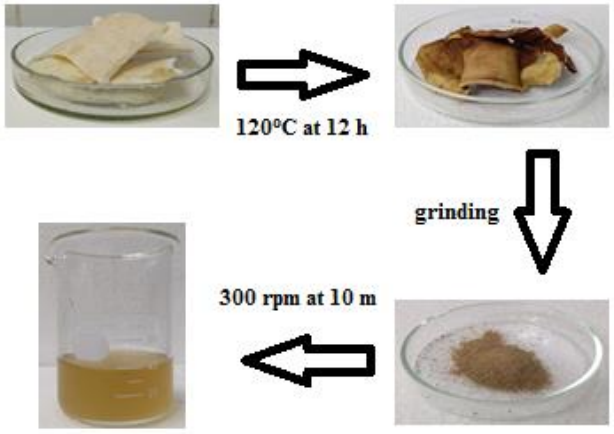

Figure 1. Schematic of carbon dots synthesis from cassava's peels using low temperature

Cassava's peels are washed and rinsed thoroughly and put in an oven at 120°C for 12 hours until the dry sample is slightly yellowish-brown in color. Dried cassava skin is ground using a blender until smooth and filtered using a sieve of 40 mesh so that the size of the cassava's peels powder is $\leq$425 μm. Cassava's peels powder is dissolved in 20 ml of water with a mass of 0.025 gr, 0.05 gr, 0.1 gr, 0.2 gr and 0.4 gr respectively and stirred using a magnetic stirrer 300 rpm for 10 minutes. That solution is filtered using filter paper $\pm$40 mesh and the C-dots colloid is obtained.

Colloidal C-dots are visually tested using a UV 405 nm laser to determine luminescence which indicated C-dots had been formed. Colloidal C-dots are characterized using a UV-Vis spectrophotometer, photoluminescence (PL) and Time Resolved Photoluminescence (TRPL).

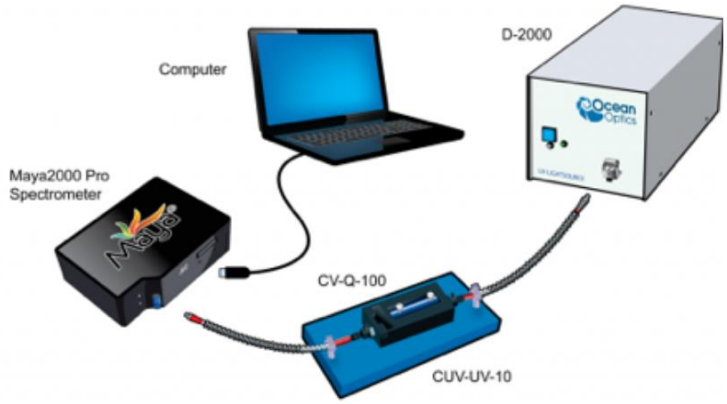

Figure 2. Optical measurement setup of absorbance

The absorbance measurements carried out using deuterium and halogen lamps as a light source and MAYARAPRO2008 Ocean Optics as a spectrometer, which can be seen in Figure 2. Measurement of PL using picosecond diode laser at a wavelength of 420 nm as the excitation source. Data is obtained using the Spectra Suite software in the form of absorbance and fluorescence spectra. Meanwhile, TRPL measurements are carried out using a laser pulse as a source of its existence with a Micro Photon Devices (MPD) detector.

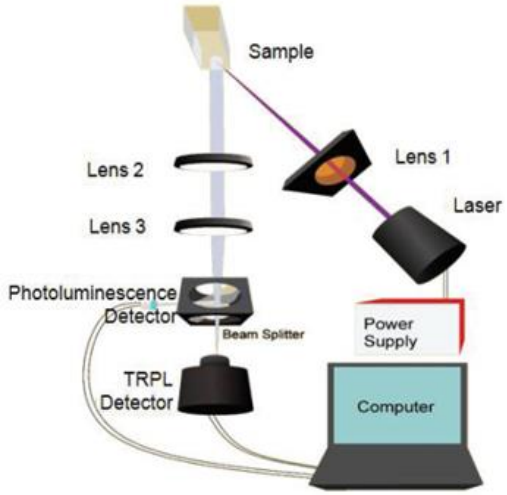

Figure 3. Optical measurement setup of photoluminescence and time-resolved photoluminescence

Photoluminescence (PL) and time-resolved photoluminescence (TRPL) measurements can be seen in Figure 3. Pico-second laser emitting light at 420 cm wavelength is used as excitation of C-dots samples. Emission of C-dots are collected and directed to two detectors, namely the photoluminescence detector and the time-resolved photoluminescence detector using a beam splitter (Isnaeni, Hanna, Pambudi, & Murdaka, 2017). The TRPL detector uses 500 nm longpass filter to block luminance under 500 nm wavelength. Data are obtained using TimeHarp 260 software.

3. Results and Discussion

C-dots obtained from the low temperature technique with variations in precursor concentrations produced physical properties of colloidal C-dots from transparent to yellow-brown under visible light, where as under UV 405 nm laser light showed luminance from cyan to green, that indicated of C-dots succesfully were synthesized. The physical properties of C-dots can be seen in **Figure 4.**

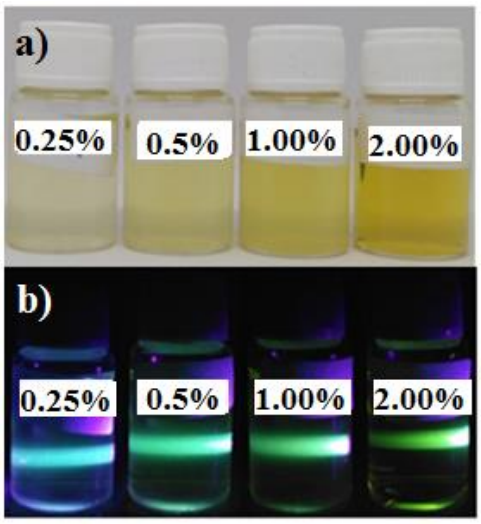

Figure 4. Physical properties of colloidal C-dots from KAS; a) under visible light; b) under the UV 405 nm laser

The optical properties of C-dots were characterized, such as the absorbance spectrums and PL spectrums using UV-Vis and PL spectrophotometers, respectively. The absorbance spectrum curve and PL of C-dots can be seen in Figure 5. and Figure 6. Respectively. In addition, electron time decay during excitation and emission conditions is characterized using time resolved photoluminescence (TRPL). The electron time decay of C-dots curves can be seen in Figure 7.

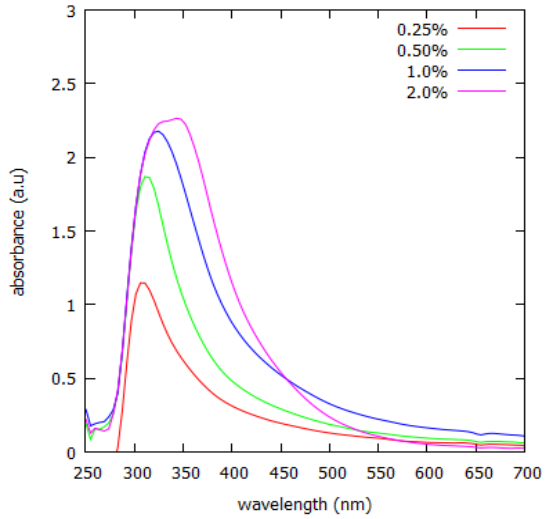

Figure 5. Absorbance curve of C-dots with variations in concentration of precursors

The absorbance peaks of C-dots is strongly influenced by the concentration of precursors during synthesis. Absorption spectrum at concentrations of 0.25%, 0.5%, 1.0% and 2.0% respectively contained at wavelength peaks of 304.67 nm, 307.97 nm, 327.72 nm and 344.15 nm which showed a transition state n-π * in the structure of aromatic bonds C = O originating from the surface of C-dots (Asha Jhonsi & Kathiravan, 2017; Han et al., 2017; Li et al., 2018; Mazrad, Kang, In, & Park, 2018). In this case, the more carbon dots are formed with increasing precursor concentrations.

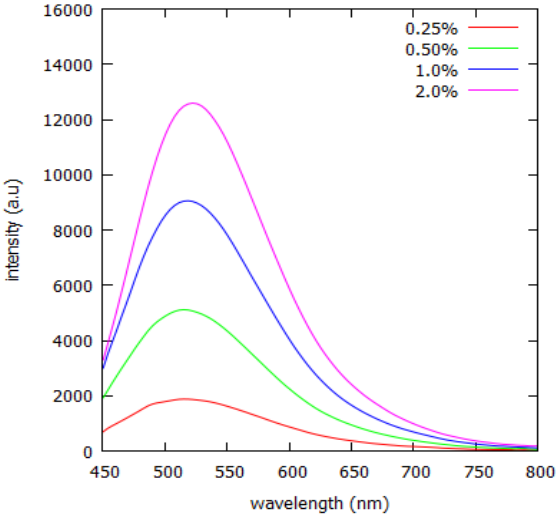

Figure 6. The PL intensity curve of C-dots with variations in concentration of precursors

The PL intensity of C-dots is strongly influenced by the concentration of precursors during synthesis. In this case, increasing the precursor concentration will increase the amount of C-dots formed. PL of C-dots are not caused by transition bandgap but surface transition state on bandgap (Yoshinaga, Iso, & Isobe, 2018). PL peaks undergo successive red shifts with increasing precursor concentrations from 0.25%, 0.5%, 1.0% and 2.0% are 509.82 nm, 515.79 nm, 519.00 nm and 524.51 nm, respectively. The red shift observed in PL peaks is ascribed to the carboxyl group and the degree of oxidation to the surface structure and not to particle size, then this PL properties are not like semiconductors quantum dots. Surface oxidation functions as the center of exciton capture has result in fluorescence associated with surface conditions. Higher oxidation levels on the C-dots surface to showed more surface defects (Ding, Yu, Wei, & Xiong, 2016). In addition, PL intensity increases by increasing the concentration of C-dots (C. Wang, Xu, & Zhang, 2015).

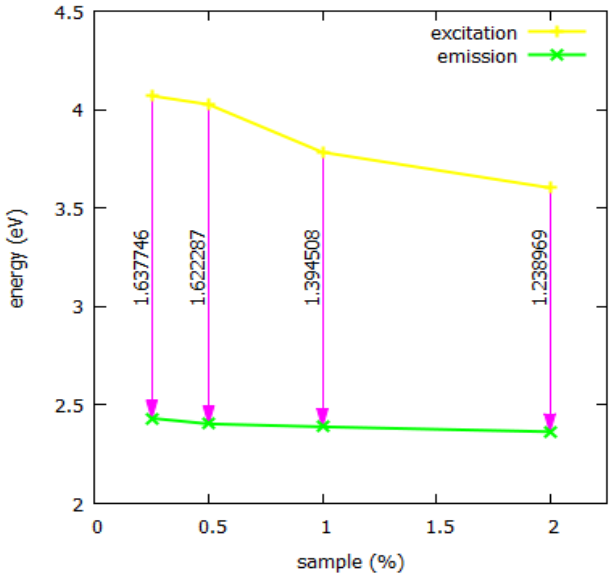

Figure 7. Stoke's shift curve of C-dots from excitation and emission states

Stoke's shift of C-dots can be analyzed through energy shifts from excitation and emissions states which can be seen in Figure 7. Energy shifts of C-dots with varying precursor concentrations from 0.25%, 0.50 %, 1.0% and 2.0% are 1.637746 eV, 1.622287 eV, 1.394508 eV and 1.238969 eV, respectively. This energy shift is caused by electron and hole interactions in separation between energy levels from valence and conduction bands. This energy transfer is commonly known as the Stoke's shift. Stoke's shift in C-dots increases with increasing precursor concentration, but is not significant. Therefore, the relaxation time of the core before carrying out emissions is very stable in aqueous solutions with an intensity that can be adjusted based on the precursor concentration.

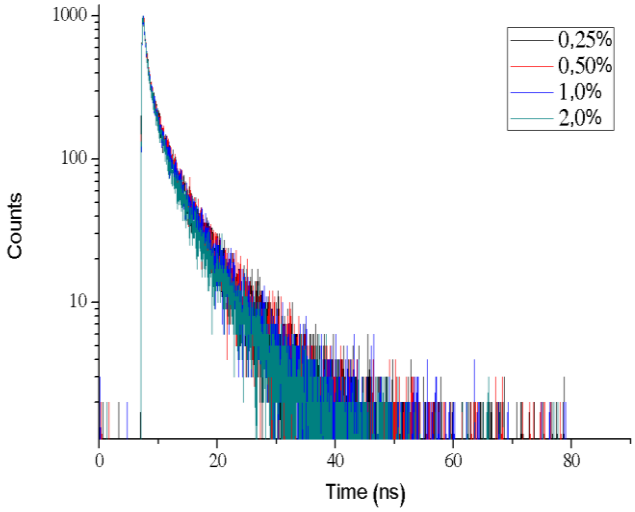

Figure 8. Electron time decay curve of C-dots with variations in concentration of precursors

Electron behavior of C-dots was also observed using TRPL with pulsed laser excitation sources. The electron time decay curve can be seen in Figure 8. This curve can be analyzed by fitted using multi-exponential decay to obtain lifetime. The Lifetime of C-dots is influenced by variations in precursor concentrations from 0.25%, 0.50%, 1.0%, and 2.0% are 3.51151877 ns, 3.75967104 ns, 3, 85196417 ns and 4,21209816 ns, respectively. A short lifetime of electron decay can show that electrons directly return to the valence band in pulsed laser excitation. Meanwhile, the longer life time of electron decay indicates that there may be additional energy levels between valence and conduction bands. Lifetime of short electron decay indicates high emission efficiency. In this case, C-dots obtained with a 2.0% precursor concentration are possible to have the best efficiency (Isnaeni et al., 2017).

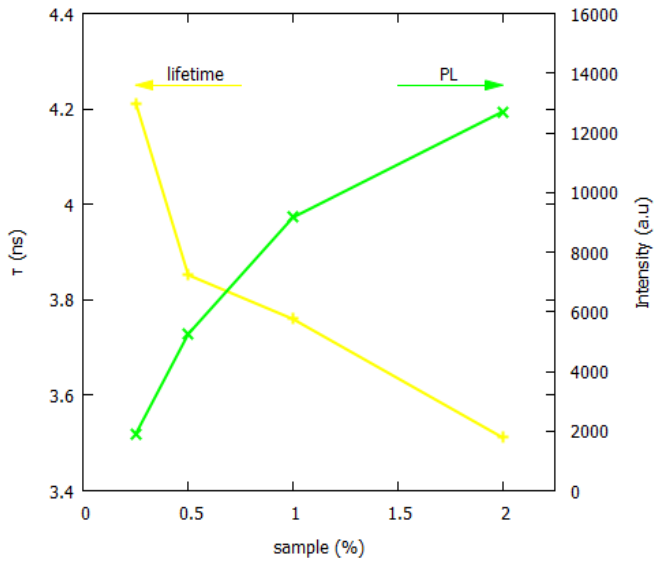

Figure 9. Correlations of lifetime and PL intensity

Photoluminescence properties of C-dots can be analyzed using correlations lifetime of C-dots and PL intensity which can be seen in Figure 9. This correlation shows that lifetimeof C-dots decreases with increasing PL intensity. The shorter lifetime of C-dots and the higher PL intensity indicate that electrons return to the valence band with high emission efficiency (Isnaeni et al., 2017). The precursor concentration also affects the relationship between lifetime and PL intensity. Although the PL mechanism and the electronic nature of C-dots are not fully understood, and it is often proposed that PL of C-dots can be associated with radiation recombination of electrons and holes trapped on the surface of C-dots (Morita, Kurusu, Kodama, & Hirayama, 2017). These results provide the potential for C-dots of cassava's peels in aqueous solutions can be applied as cellular bioimaging in vivo and in vitro and biosensing metal ions and salts. However, additional optical measurements are needed to support our findings.

4. Conclusion

Cassava's peels has been successfully synthesized into C-dots using green synthesis methods with low temperature. The concentration of precursors in synthesis affects the optical properties of C-dots. C-dots samples with a 2.0% precursor concentration have the best emission efficiency. This precursor concentration is assumed to play a role in the behavior of the optical properties of C-dots because of their molecular density. The behavior of C-dots optical properties is dominated by the electron transition n-π * in the structure of C = O aromatic bonds originating from the surface of C-dots.

Acknowledgments

Thank you to the laser research group at the Physics Research Center of the Indonesian Institute of Sciences which has given permission to conduct research in the laser laboratory.

Refference

Asha Jhonsi, M., & Kathiravan, A. (2017). Photoinduced interaction of arylamine dye with carbon quantum dots ensued from centella asiatica. *Journal of Luminescence*, *192*, 321–327. https://doi.org/10.1016/j.jlumin.2017.06.056

Baker, S. N., & Baker, G. A. (2010). Luminescent carbon nanodots: Emergent nanolights. *Angewandte Chemie - International Edition*, *49*(38), 6726–6744. https://doi.org/10.1002/anie.200906623

Dimos, K. (2016). Carbon quantum dots: Surface passivation and functionalization. *Current Organic Chemistry*, *20*, 682–695. https://doi.org/10.2174/1385272819666150730220948

Ding, H., Yu, S. B., Wei, J. S., & Xiong, H. M. (2016). Full-color light-emitting carbon dots with a surface-state-controlled luminescence mechanism. *ACS Nano*, *10*(1), 484–491. https://doi.org/10.1021/acsnano.5b05406

Fatimah, S., Isnaeni, & Tahir, D. (2018). Assisted surface-state recombination of orange-peel carbon nanodots in various matrices. *Makara J. Sci*, *22*(1), 29–34. https://doi.org/10.7454/mss.v22.i1.8301

Goryacheva, I. Y., Sapelkin, A. V., & Sukhorukov, G. B. (2017). Carbon nanodots: Mechanisms of photoluminescence and principles of application. *TrAC - Trends in Analytical Chemistry*, *90*, 27–37. https://doi.org/10.1016/j.trac.2017.02.012

Han, S., Chang, T., Zhao, H., Du, H., Liu, S., Wu, B., & Qin, S. (2017). Cultivating fluorescent flowers with highly luminescent carbon dots fabricated by a double passivation method. *Nanomaterials*, *7*(7), 176. https://doi.org/10.3390/nano7070176

Hassan, M., Gomes, V. G., Dehghani, A., & Ardekani, S. M. (2018). Engineering carbon quantum dots for photomediated theranostics. *Nano Research*, *11*(1), 1–41. https://doi.org/10.1007/s12274-017-1616-1

Hola, K., Zhang, Y., Wang, Y., Giannelis, E. P., Zboril, R., & Rogach, A. L. (2014). Carbon dots-Emerging light emitters for bioimaging, cancer therapy and optoelectronics. *Nano Today*, *9*(5), 590–603. https://doi.org/10.1016/j.nantod.2014.09.004

Hu, Q., Gong, X., Liu, L., & Choi, M. M. F. (2017). Characterization and analytical separation of fluorescent carbon nanodots. *Journal of Nanomaterials*, 30–37. https://doi.org/10.1155/2017/1804178

Huang, H., Lv, J. J., Zhou, D. L., Bao, N., Xu, Y., Wang, A. J., & Feng, J. J. (2013). One-pot green synthesis of nitrogen-doped carbon nanoparticles as fluorescent probes for mercury ions. *RSC Advances*, *3*(44), 21691–21696. https://doi.org/10.1039/c3ra43452d

Isnaeni, Hanna, M. Y., Pambudi, A. A., & Murdaka, F. H. (2017). Influence of ablation wavelength and time on optical properties of laser ablated carbon dots. *AIP Conference Proceedings*, *1801*(020001), 1–5. https://doi.org/10.1063/1.4973079

Isnaeni, Rahmawati, I., Intan, R., & Zakaria, M. (2018). Photoluminescence study of carbon dots from ginger and galangal herbs using microwave technique. *Journal of Physics: Conf. Series*, (985), 1–6. https://doi.org/10.1088/1742-6596/985/1/012004

Jaleel, J. A., & Pramod, K. (2018). Artful and multifaceted applications of carbon dot in biomedicine. *Journal of Controlled Release*, *269*, 302–321. https://doi.org/10.1016/j.jconrel.2017.11.027

Li, Q., Zhou, M., Yang, M., Yang, Q., Zhang, Z., & Shi, J. (2018). Induction of long-lived room temperature phosphorescence of carbon dots by water in hydrogen-bonded matrices. *Nature Communications*, *9*(734), 1–8. https://doi.org/10.1038/s41467-018-03144-9

Liu, Y., Zhao, Y., & Zhang, Y. (2014). One-step green synthesized fluorescent carbon nanodots from bamboo leaves for copper (II) ion detection. *Sensors and Actuators, B: Chemical*, *196*, 647–652. https://doi.org/10.1016/j.snb.2014.02.053

Ma, X., Dong, Y., Sun, H., & Chen, N. (2017). Highly fluorescent carbon dots from peanut shells as potential probes for copper ion: The optimization and analysis of the synthetic process. *Materials Today Chemistry*, *5*, 1–10.

https://doi.org/10.1016/j.mtchem.2017.04.004

Mazrad, Z. A. I., Kang, E. B., In, I., & Park, S. Y. (2018). Preparation of carbon dot-based ratiometric fluorescent probes for cellular imaging from curcuma longa. *Luminescence*, *33*(1), 40–46. https://doi.org/10.1002/bio.3370

Morita, K., Kurusu, S., Kodama, H., & Hirayama, N. (2017). Effect of the elemental composition of precursors from amino acids and their binary mixtures on the photoluminescent intensity of carbon nanodots. *Analytical Sciences*, *33*, 1461–1464. https://doi.org/10.2116/analsci.33.1461

Neto, A. H. C., Guinea, F., Peres, N. M. R., Novoselov, K. S., & Geim, A. K. (2009). The electronic properties of graphene. *Reviews of Modern Physics*, *81*, 109–162. https://doi.org/10.1103/RevModPhys.81.109

Ngu, P. Z. Z., Chia, S. P. P., Fong, J. F. Y., & Ng, S. M. (2016). Synthesis of carbon nanoparticles from waste rice husk used for the optical sensing of metal ions. *New Carbon Materials*, *31*(2), 135–143. https://doi.org/10.1016/S1872-5805(16)60008-2

Shen, J., Shang, S., Chen, X., Wang, D., & Cai, Y. (2017). Facile synthesis of fluorescence carbon dots from sweet potato for Fe^{3+} sensing and cell imaging. *Materials Science and Engineering C*, *76*, 856–864. https://doi.org/10.1016/j.msec.2017.03.178

Varisco, M., Zufferey, D., Ruggi, A., Zhang, Y., Erni, R., & Mamula, O. (2017). Synthesis of hydrophilic and hydrophobic carbon quantum dots from waste of wine fermentation. *Royal Society Open Science*, *4*(12), 170900. https://doi.org/10.1098/rsos.170900

Wang, C., Xu, Z., & Zhang, C. (2015). Polyethyleneimine-functionalized fluorescent carbon dots: Water stability, pH sensing, and cellular imaging. *ChemNanoMat*, *1*(2), 122–127. https://doi.org/10.1002/cnma.201500009

Wang, R., Lu, K.-Q., Tang, Z.-R., & Xu, Y.-J. (2017). Recent progress in carbon quantum dots: synthesis, properties and applications in photocatalysis. *J. Mater. Chem. A*, *5*(8), 3717–3734. https://doi.org/10.1039/C6TA08660H

Yin, B., Deng, J., Peng, X., Long, Q., Zhao, J., Lu, Q., … Yao, S. (2013). Green synthesis of carbon dots with down- and up-conversion fluorescent properties for sensitive detection of hypochlorite with a dual-readout assay. *Analyst*, *138*(21), 6551–6557. https://doi.org/10.1039/c3an01003a

Yoshinaga, T., Iso, Y., & Isobe, T. (2018). Particulate, structural, and optical properties of D-glucose-derived carbon dots synthesized by microwave-assisted hydrothermal treatment. *ECS Journal of Solid State Science and Technology*, *7*(1), R3034–R3039. https://doi.org/10.1149/2.0091801jss